Title

Detection of doxorubicin-induced apoptosis of leukemic T-lymphocytes by laser tweezers Raman spectroscopy

Journal

Biomedical Optics Express, 1(4)

ISSN

2156-7085

Authors

Moritz, Tobias J
Taylor, Douglas S
Krol, Denise M
et al.

Publication Date

2010-11-01

DOI

10.1364/boe.1.001138

Peer reviewed

Detection of doxorubicin-induced apoptosis of leukemic T-lymphocytes by laser tweezers Raman spectroscopy

Tobias J. Moritz,[1,2] Douglas S. Taylor,[1,3] Denise M. Krol,[2,4] John Fritch,[1] and James W. Chan[1,*]

[1]*NSF Center for Biophotonics Science and Technology, University of California, Davis, 2700 Stockton Blvd Suite 1400, Sacramento, CA 95817, USA*
[2]*Biophysics Graduate Group, University of California, Davis, One Shields Ave, Davis, CA 95616, USA*
[3]*Department of Pediatrics, University of California Davis Medical Center, 2516 Stockton Blvd, Sacramento, CA 95817, USA*
[4]*Department of Applied Science, University of California, Davis, One Shields Ave, Davis, CA 95616, USA*
**jwjchan@ucdavis.edu*

Abstract: Laser tweezers Raman spectroscopy (LTRS) was used to acquire the Raman spectra of leukemic T lymphocytes exposed to the chemotherapy drug doxorubicin at different time points over 72 hours. Changes observed in the Raman spectra were dependent on drug exposure time and concentration. The sequence of spectral changes includes an intensity increase in lipid Raman peaks, followed by an intensity increase in DNA Raman peaks, and finally changes in DNA and protein (phenylalanine) Raman vibrations. These Raman signatures are consistent with vesicle formation, cell membrane blebbing, chromatin condensation, and the cytoplasm of dead cells during the different stages of drug-induced apoptosis. These results suggest the potential of LTRS as a real-time single cell tool for monitoring apoptosis, evaluating the efficacy of chemotherapeutic treatments, or pharmaceutical testing.

OCIS codes: (300.6450) Spectroscopy, Raman; (170.4520) Optical confinement and manipulation; (170.1530) Cell analysis; (140.7010) Laser trapping; (290.5860) Scattering, Raman

References and links

1. R. C. Taylor, S. P. Cullen, and S. J. Martin, "Apoptosis: controlled demolition at the cellular level," Nat. Rev. Mol. Cell Biol. **9**(3), 231–241 (2008).
2. S. W. Lowe, and A. W. Lin, "Apoptosis in cancer," Carcinogenesis **21**(3), 485–495 (2000).
3. J. C. Reed, "Dysregulation of apoptosis in cancer," J. Clin. Oncol. **17**(9), 2941–2953 (1999).
4. J. F. Kerr, C. M. Winterford, and B. V. Harmon, "Apoptosis. Its significance in cancer and cancer therapy," Cancer **73**(8), 2013–2026 (1994).
5. T. G. Cotter, "Apoptosis and cancer: the genesis of a research field," Nat. Rev. Cancer **9**(7), 501–507 (2009).
6. M. H. Cheok, W. Yang, C. H. Pui, J. R. Downing, C. Cheng, C. W. Naeve, M. V. Relling, and W. E. Evans, "Treatment-specific changes in gene expression discriminate in vivo drug response in human leukemia cells," Nat. Genet. **34**(1), 85–90 (2003).
7. R. A. Nagourney, "Ex vivo programmed cell death and the prediction of response to chemotherapy," Curr. Treat. Options Oncol. **7**(2), 103–110 (2006).
8. L. Möllgård, U. Tidefelt, B. Sundman-Engberg, C. Löfgren, and C. Paul, "In vitro chemosensitivity testing in acute non lymphocytic leukemia using the bioluminescence ATP assay," Leuk. Res. **24**(5), 445–452 (2000).
9. J. M. Sargent, and C. G. Taylor, "Appraisal of the MTT assay as a rapid test of chemosensitivity in acute myeloid leukaemia," Br. J. Cancer **60**(2), 206–210 (1989).
10. F. Buccisano, L. Maurillo, A. Spagnoli, M. I. D. Principe, E. Ceresoli, F. L. Coco, W. Arcese, S. Amadori, and A. Venditti, "Monitoring of minimal residual disease in acute myeloid leukemia," Curr. Opin. Oncol. **21**(6), 582–588 (2009).
11. J. Donadieu, and C. Hill, "Early response to chemotherapy as a prognostic factor in childhood acute lymphoblastic leukaemia: a methodological review," Br. J. Haematol. **115**(1), 34–45 (2001).
12. C. S. Mulvey, C. A. Sherwood, and I. J. Bigio, "Wavelength-dependent backscattering measurements for quantitative real-time monitoring of apoptosis in living cells," J. Biomed. Opt. **14**(6), 064013 (2009).

#135484 - $15.00 USD Received 29 Sep 2010; revised 6 Oct 2010; accepted 7 Oct 2010; published 11 Oct 2010

13. J. Chan, S. Fore, S. Wachsmann-Hogiu, and T. Huser, "Raman spectroscopy and microscopy of individual cells and cellular components," Laser Photonics Rev. **2**(5), 325–349 (2008).
14. R. Buckmaster, F. Asphahani, M. Thein, J. Xu, and M. Zhang, "Detection of drug-induced cellular changes using confocal Raman spectroscopy on patterned single-cell biosensors," Analyst (Lond.) **134**(7), 1440–1446 (2009).
15. H. Yao, Z. Tao, M. Ai, L. Peng, G. Wang, B. He, and Y. Li, "Raman spectroscopic analysis of apoptosis of single human gastric cancer cells," Vib. Spectrosc. **50**(2), 193–197 (2009).
16. C. A. Owen, J. Selvakumaran, I. Notingher, G. Jell, L. L. Hench, and M. M. Stevens, "In vitro toxicology evaluation of pharmaceuticals using Raman micro-spectroscopy," J. Cell. Biochem. **99**(1), 178–186 (2006).
17. N. Uzunbajakava, A. Lenferink, Y. Kraan, E. Volokhina, G. Vrensen, J. Greve, and C. Otto, "Nonresonant confocal Raman imaging of DNA and protein distribution in apoptotic cells," Biophys. J. **84**(6), 3968–3981 (2003).
18. A. Zoladek, F. C. Pascut, P. Patel, and I. Notingher, "Non-invasive time-course imaging of apoptotic cells by confocal Raman micro-spectroscopy," J. Raman Spectroscopy, n/a-n/a (2010).
19. J. W. Chan, A. P. Esposito, C. E. Talley, C. W. Hollars, S. M. Lane, and T. Huser, "Reagentless identification of single bacterial spores in aqueous solution by confocal laser tweezers Raman spectroscopy," Anal. Chem. **76**(3), 599–603 (2004).
20. C. G. Xie, M. A. Dinno, and Y. Q. Li, "Near-infrared Raman spectroscopy of single optically trapped biological cells," Opt. Lett. **27**(4), 249–251 (2002).
21. T. J. Moritz, J. A. Brunberg, D. M. Krol, S. Wachsmann-Hogiu, S. M. Lane, and J. W. Chan, "Characterization of FXTAS related isolated intranuclear protein inclusions using laser tweeezers Raman spectroscopy," J. Raman Spectroscopy **40**(2009).
22. C. A. Lieber, and A. Mahadevan-Jansen, "Automated method for subtraction of fluorescence from biological Raman spectra," Appl. Spectrosc. **57**(11), 1363–1367 (2003).
23. I. Notingher, G. Jell, P. L. Notingher, I. Bisson, O. Tsigkou, J. M. Polak, M. M. Stevens, and L. L. Hench, "Multivariate analysis of Raman spectra for in vitro non-invasive studies of living cells," J. Mol. Struct. **744-747**, 179–185 (2005).
24. J. W. Chan, D. S. Taylor, T. Zwerdling, S. M. Lane, K. Ihara, and T. Huser, "Micro-Raman spectroscopy detects individual neoplastic and normal hematopoietic cells," Biophys. J. **90**(2), 648–656 (2006).
25. M. Niepel, S. L. Spencer, and P. K. Sorger, "Non-genetic cell-to-cell variability and the consequences for pharmacology," Curr. Opin. Chem. Biol. **13**(5-6), 556–561 (2009).
26. C. Ferraro-Peyret, L. Quemeneur, M. Flacher, J. P. Revillard, and L. Genestier, "Caspase-independent phosphatidylserine exposure during apoptosis of primary T lymphocytes," J. Immunol. **169**(9), 4805–4810 (2002).
27. M. L. Coleman, E. A. Sahai, M. Yeo, M. Bosch, A. Dewar, and M. F. Olson, "Membrane blebbing during apoptosis results from caspase-mediated activation of ROCK I," Nat. Cell Biol. **3**(4), 339–345 (2001).
28. S. Gamen, A. Anel, P. Lasierra, M. A. Alava, M. J. Martinez-Lorenzo, A. Piñeiro, and J. Naval, "Doxorubicin-induced apoptosis in human T-cell leukemia is mediated by caspase-3 activation in a Fas-independent way," FEBS Lett. **417**(3), 360–364 (1997).
29. D. C. Dartsch, A. Schaefer, S. Boldt, W. Kolch, and H. Marquardt, "Comparison of anthracycline-induced death of human leukemia cells: programmed cell death versus necrosis," Apoptosis **7**(6), 537–548 (2002).
30. S. Gamen, A. Anel, P. Pérez-Galán, P. Lasierra, D. Johnson, A. Piñeiro, and J. Naval, "Doxorubicin treatment activates a Z-VAD-sensitive caspase, which causes deltapsim loss, caspase-9 activity, and apoptosis in Jurkat cells," Exp. Cell Res. **258**(1), 223–235 (2000).
31. S. Wesselborg, I. H. Engels, E. Rossmann, M. Los, and K. Schulze-Osthoff, "Anticancer drugs induce caspase-8/FLICE activation and apoptosis in the absence of CD95 receptor/ligand interaction," Blood **93**(9), 3053–3063 (1999).
32. A. A. Sokolovskaya, T. N. Zabotina, D. Y. Blokhin, Z. G. Kadagidze, and A. Y. Baryshnikov, "Comparative analysis of apoptosis induced by various anticancer drugs in Jurkat cells," Exp. Oncol. **23**, 46–50 (2001).
33. G. E. N. Kass, J. E. Eriksson, M. Weis, S. Orrenius, and S. C. Chow, "Chromatin condensation during apoptosis requires ATP," Biochem. J. **318**(Pt 3), 749–752 (1996).
34. V. L. Johnson, S. C. W. Ko, T. H. Holmstrom, J. E. Eriksson, and S. C. Chow, "Effector caspases are dispensable for the early nuclear morphological changes during chemical-induced apoptosis," J. Cell Sci. **113**(Pt 17), 2941–2953 (2000).
35. Y. Takai, T. Masuko, and H. Takeuchi, "Lipid structure of cytotoxic granules in living human killer T lymphocytes studied by Raman microspectroscopy," Biochim. Biophys. Acta **1335**(1-2), 199–208 (1997).
36. J. W. Chan, D. S. Taylor, S. M. Lane, T. Zwerdling, J. Tuscano, and T. Huser, "Nondestructive identification of individual leukemia cells by laser trapping Raman spectroscopy," Anal. Chem. **80**(6), 2180–2187 (2008).
37. R. D. Snook, T. J. Harvey, E. Correia Faria, and P. Gardner, "Raman tweezers and their application to the study of singly trapped eukaryotic cells," Integr Biol (Camb) **1**(1), 43–52 (2009).
38. G. J. Puppels, J. H. F. Olminkhof, G. M. J. Segers-Nolten, C. Otto, F. F. M. de Mul, and J. Greve, "Laser irradiation and Raman spectroscopy of single living cells and chromosomes: sample degradation occurs with 514.5 nm but not with 660 nm laser light," Exp. Cell Res. **195**(2), 361–367 (1991).
39. P. R. T. Jess, V. Garcés-Chávez, D. Smith, M. Mazilu, L. Paterson, A. Riches, C. S. Herrington, W. Sibbett, and K. Dholakia, "Dual beam fibre trap for Raman micro-spectroscopy of single cells," Opt. Express **14**(12), 5779–5791 (2006).
40. A. Y. Lau, L. P. Lee, and J. W. Chan, "An integrated optofluidic platform for Raman-activated cell sorting," Lab Chip **8**(7), 1116–1120 (2008).

#135484 - $15.00 USD Received 29 Sep 2010; revised 6 Oct 2010; accepted 7 Oct 2010; published 11 Oct 2010

41. K. Ramser, J. Enger, M. Goksör, D. Hanstorp, K. Logg, and M. Käll, "A microfluidic system enabling Raman measurements of the oxygenation cycle in single optically trapped red blood cells," Lab Chip **5**(4), 431–436 (2005).
42. K. Ramser, W. Wenseleers, S. Dewilde, S. Van Doorslaer, and L. Moens, "The combination of resonance Raman spectroscopy, optical tweezers and microfluidic systems applied to the study of various heme-containing single cells," Spectroscopy **22**, 287–295 (2008).
43. K. Ramser, W. Wenseleers, S. Dewilde, S. Van Doorslaer, L. Moens, and D. Hanstorp, "Micro-resonance Raman study of optically trapped Escherichia coli cells overexpressing human neuroglobin," J. Biomed. Opt. **12**(4), 044009 (2007).
44. R. Liu, D. S. Taylor, D. L. Matthews, and J. W. Chan, "Parallel analysis of individual biological cells using multifocal laser tweezers Raman spectroscopy," Appl. Spectrosc. (to be published).

1. Introduction

Apoptosis is the natural biological process of programmed cell death in which extracellular or intracellular cell signals trigger internal cellular machinery to induce self-destruction of the cell [1]. Characteristic changes in cell morphology associated with apoptosis include blebbing, cell shrinkage, nuclear fragmentation, and chromatin condensation. Apoptosis plays an important role in cancer, both in its development and its treatment [2]. Dysregulation of the normal apoptotic pathway impairs the cell's ability to undergo apoptosis [3–5]. This increases the likelihood of cancerous or diseased cells being formed as the cell replicates and passes genetic instabilities and gene mutations to its progeny. Defective apoptotic pathways also lead to the expansion of neoplastic cell populations due to the extension of cell life span. Apoptosis is also an important process in cancer treatment, since many chemotherapy drugs kill cancer cells by inducing apoptosis via different pathways.

Current treatment of cancer is largely empirical and derived from the association of surrogate patient or disease markers with observed patient outcome. Chemotherapy is, therefore, chosen for an individual patient based on protocols developed from observations from prior clinical studies on other patients. This paradigm precludes the possibility of predicting either those cancers that will subsequently fail therapy or those that are over treated using a single regimen applied to a broad population of patients. The concept of *in vitro* assay-directed, patient-specific therapy [6–9] is based on the premise that an individual's cancer cells are unique, and therefore will be best managed using a personalized chemotherapy regimen. An *in-vitro* chemosensitivity assay that can test the response of a patient's cell to different drugs to guide treatment and monitor therapy has the potential to improve the management of the disease by both improving efficacy and limiting unnecessary toxicity. Early stage detection of cellular response to treatment and applicability to samples containing small cell numbers are also desired in a diagnostic method [10,11].

A variety of apoptotic assays such as 3-(4,5-dimethyl-thiazol-2-yl)-2,5-diphenyl-tetrazolium bromide (MTT), membrane, ATP, and protein based assays, which measure energy metabolism, membrane integrity, protein synthesis, enzymatic activity, or ATP content as endpoints related to cellular function associated with cell survival [7], have been investigated for *in-vitro* chemosensitivity testing, but their *in-vivo* correlation to accurately predict patient outcomes remains uncertain. Many of these assays are invasive and destructive, which prevent cellular dynamics associated with apoptosis from being monitored in individual living cells. Similarly, antibody based fluorescence imaging can only provide single endpoint measurements of the cell because they require cell fixation and permeabilization, which render the cells nonviable. Although standard white light microscopy (e.g. brightfield, phase contrast) does permit noninvasive morphological analysis of cells, it provides no biochemical information needed to study apoptosis at the molecular level. A new method based on elastic light scattering spectroscopy has been developed for real-time apoptosis monitoring in living cells [12] but it also provides no direct biochemical information. Therefore, new *in-vitro* chemosensitivity assays are needed that could provide new apoptotic markers for improving therapy monitoring and guiding patient treatment.

Micro-Raman spectroscopy is an attractive optical technique for monitoring cell-drug interactions given its unique ability to provide biochemical information without the need to perturb the cell with chemical fixatives, labeling, or genetic modification. Detection of

#135484 - $15.00 USD Received 29 Sep 2010; revised 6 Oct 2010; accepted 7 Oct 2010; published 11 Oct 2010

Stokes-shifted inelastically scattered photons generates a Raman spectrum, a molecular fingerprint providing highly multiplexed biochemical information of DNA, RNA, proteins, and lipid content. While Raman spectroscopy has been used extensively for the characterization, identification, and discrimination of different cell types and to investigate cellular processes [13], it has, to a lesser extent, been applied for the study of cellular apoptosis induced by chemotherapy agents [14–18]. Here, we apply laser tweezers Raman spectroscopy (LTRS) [19,20], a variation of micro-Raman spectroscopy in which a tightly focused laser beam is used to both optically trap single suspension cells within the laser focus while probing the molecular bonds by Raman scattering, to monitor the cellular response of leukemia cells to the chemotherapeutical drug doxorubicin, with the aim of establishing time-resolved Raman spectroscopic markers of white blood cells undergoing different phases of programmed cell death.

2. Materials and methods

2.1 Laser tweezers Raman spectroscopy system

The LTRS system used in this study has been described previously [21]. A single laser beam from a 785 nm CW diode laser (80mW, CrystaLaser) coupled into an inverted microscope (Olympus IX71) was used to trap individual cells and generate Raman spectra. An optical isolator (Thorlabs, IO-5-780-HP) placed in front of the laser beam was used to stabilize the laser wavelength. A 10x Kepler-telescope expanded the beam to overfill the back aperture of the microscope objective (Olympus 60x/1.2 NA water immersion) in order to generate a tightly focused laser beam for stable optical trapping of the cells. A laser spot of about 1 μm diameter and 25 mW at the sample was achieved. The Raman signals from the probed cells were detected by a fiber-coupled spectrograph (Acton, SpectraPro 2300i) equipped with a 600 grooves/mm grating and a thermoelectrically cooled CCD camera (PI/Acton, PIXIS 100).

2.2 Cell culture

Jurkat T cells were obtained from American Type Culture Collection (Jurkat clone E6-1, ATCC, Rockville, MD), a commonly used model system of T-cell leukemia, and maintained in culture with RPMI-1640 medium (ATCC) containing the supplements HEPES, sodium pyruvate, L-glutamine, 10% fetal bovine serum (GIBCO 10437), and 1 Vol% of the antibiotics Penicillin G (100 units per mL)/Streptomycin (100 μg per mL) (Gibco 1552) at a temperature of 37°C, a relative humidity of 90%, and 5% carbon dioxide content in air. Cell density was maintained between 7.5×10^5 and 2.5×10^6 cells per ml.

2.3 Drug exposure of leukemia cells

Jurkat T cells in culture were continuously exposed to 0.1 μM and 0.5 μM concentrations of the chemotherapeutical drug Doxorubicin (Adriamycin). The drug-exposed cells were kept in the incubator during the entire time of the experiment (72 hours) and 80 μl samples were extracted from the culture flask every 24h for Raman spectroscopic interrogation. The 80 μl cell sample (cells in media and drug) was diluted with 140 μl phosphate buffered saline (PBS) solution prior to Raman analysis.

2.4 Raman spectroscopic measurements and data processing

Drug-exposed cell samples diluted in PBS solution were placed into an investigation well (silicon isolator, Grace Bio-labs) on a poly-HEMA (2-hydroxyethyl methacrylate) coated, quartz microscope cover slip. The poly-HEMA coating was applied to the cover slip through spin coating (50 μl of 2% poly-HEMA in ethanol at 4200 rpm for 20s) to prevent the cells from adhering to the cover slip. Raman spectra of 30 individual, optically trapped Jurkat cells were recorded for cell samples at each time point (at 24, 48, 72 hours). The spectral acquisition time for each cell was 60s. Each spectrum was background corrected by subtracting the solvent background followed by an additional baseline correction using an iterative polynomial fitting approach [22] and normalized to the total area under the curve.

#135484 - $15.00 USD Received 29 Sep 2010; revised 6 Oct 2010; accepted 7 Oct 2010; published 11 Oct 2010

Principal component analysis (PCA) [23,24] was also performed on the Raman data set to reduce dimensionality while retaining maximum data variance to identify discrete data groups plotted in two-dimensional principal component scatter plots. All programs for data processing were programmed using MATLAB software.

3. Results and discussion

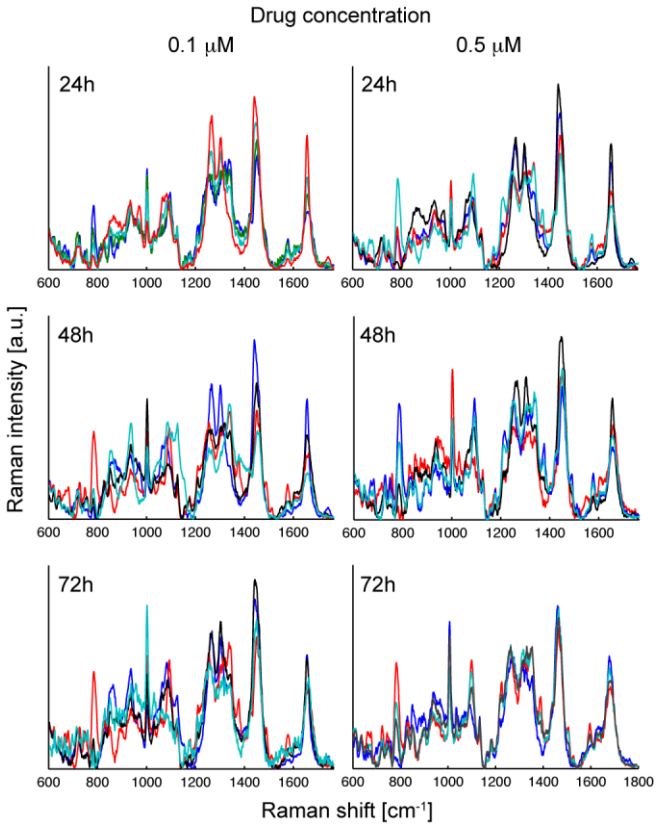

Fig. 1. Raman spectra of individual Jurkat cells after different times of drug exposure. Spectral data are shown (only 4 out of 30 per data point) for continuous doxorubicin exposure after 24h, 48h, and 72h for drug concentrations of 0.1 μM and 0.5 μM.

Figure 1 shows Raman spectra of individual Jurkat cells exposed to 0.1 μM and 0.5 μM doxorubicin, taken after 24h, 48h and 72h of initial exposure. Only 4 of the 30 Raman spectra are shown for each drug concentration and time point in order to maintain clarity in the figure. It is immediately clear that there is significant heterogeneity in the Raman spectra within each drug exposure time point, presumably reflecting the variability in drug sensitivity and cellular response due to the stochastic nature of cellular biochemical reactions [25]. This significant variability in the Raman spectra made it difficult to directly compare the spectral data groups at each time point to determine the spectral changes that occur as a function of drug exposure time. Rather, an alternative approach was used to identify Raman spectroscopic changes that correlate with different phases of drug induced cell response whereby PCA was performed on the entire Raman spectra data set inclusive of all time points for each drug concentration. Figure 2 is a scatter plot of principal component 2 (PC2) versus principal component 1 (PC1) for Jurkat cells exposed to 0.5 μM doxorubicin. The PCA results reveal that drug exposed cells undergo spectral changes leading to the formation of distinct groups in the scatter plot. By visual inspection, four clusters of Raman spectra can be delineated in the scatter plot, which are circled in Fig. 2 for clarity. Note that the boundaries of these circles were defined by grouping data points based on similarities in their Raman spectral features (to be discussed

#135484 - $15.00 USD Received 29 Sep 2010; revised 6 Oct 2010; accepted 7 Oct 2010; published 11 Oct 2010

below in Fig. 4). In general, there appears to be a trend of the clusters grouping according to drug exposure time. Jurkat cells unexposed to the drug and sampled over 72 hours are also plotted (blue circles), which serve as a control group that defines the region in the plot corresponding to cells exhibiting minimal spectral changes. The tight clustering of these points (circled in blue) excludes the possibility that cell culturing over 72 hours without the addition of fresh culture medium is responsible for the spectral changes observed in the drug exposed cells.

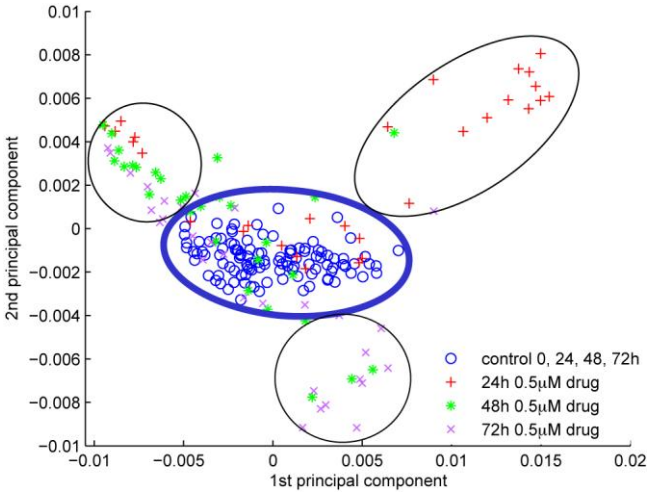

Fig. 2. PCA scatter plot of Raman spectra of control (no drug exposure) and drug exposed (0.5 μM doxorubicin) Jurkat cells over 72 h. Three groups are visible (circled in black) that are located apart from the control cell group (circled in blue).

To further elucidate the sequence in which drug induced changes in the Raman spectra occur and to explore the dependence of these changes on drug concentration, Raman spectra of cells exposed to 0.1 and 0.5 μM doxorubicin from 24 to 72 h were simultaneously analyzed by PCA to generate the scatter plot (Fig. 3). Raman spectra of cells exposed to 0.1 μM after 24 hours are strongly localized in *only* one cluster (other than the control group circled in blue) labeled group 1 in Fig. 3. This group signifies the first detectable spectral changes that occur. Spectra of cells after 48 h of drug (0.1 μm) exposure produce the second distinct cluster (group 2) in the PCA plot, based on the observation that these points were found in both the control group, group 1, and extended to group 2. Group 3 of the PCA plot was identified by the fact that spectra taken after 24 h of cell exposure to 0.5 μM drug were located only in groups 1 and 2 but group 3 only contains spectra taken after 48 and 72 h (0.5 μM).

The results in Fig. 3 also illustrate that a relationship exists between the temporal evolution of the spectral changes and the drug concentration. While 24 h of exposure to 0.1 μM doxorubicin results in cells clustering only in group 1 (other than the control), exposure to 0.5 μM drug for the same duration leads to clustering of cells in both groups 1 and 2. This same trend is observed in the 48 h data, which shows that cells exposed to 0.1 μM drug leads to clustering in groups 1 and 2, while 0.5 μM drug exposure leads to localization in groups 2 and 3. These observations indicate that Raman spectroscopy has the sensitivity to detect the faster drug response of cells exposed to higher drug concentrations leading eventually to cell death. Also note that the overlap in the data points between the 3 groups observed in both PCA plots (Fig. 2 and 3) reflects the significant cell-to-cell variability in the drug response behavior of individual cells. The overlap of some drug exposed cells and the control cells also indicates that not all drug exposed cells showed a change in their spectra, suggesting that some of these cells may have a slower drug response or may exhibit a drug-resistant phenotype. These results reinforce the importance of measuring single cells to capture heterogeneity.

#135484 - $15.00 USD Received 29 Sep 2010; revised 6 Oct 2010; accepted 7 Oct 2010; published 11 Oct 2010

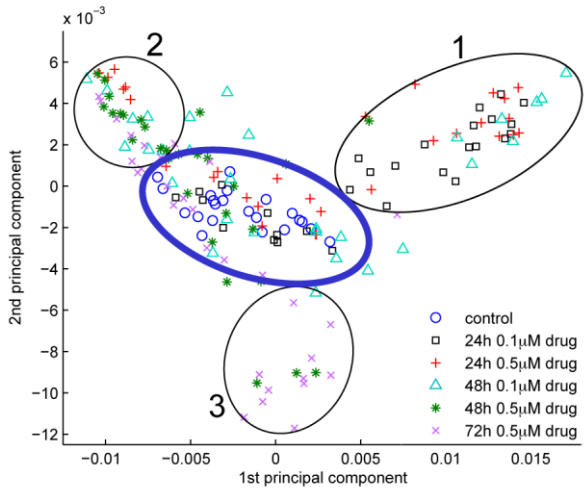

Fig. 3. PCA scatter plot of 0.1 and 0.5 μM drug exposed and control (no drug exposure) cells at 24, 48, and 72 h. Groups 1, 2, and 3 indicate the sequence in which these clusters are formed. A dependence between the temporal evolution of the spectral changes and drug concentration is also observed based on the distribution of data points in each of the groups.

Figure 4 shows the average Raman spectra of all cells from each of the three groups in the PCA scatter plots for both drug concentrations. It should be emphasized that this analysis no longer groups the data by the exposure time of the cells to the drugs, due to the cell-to-cell heterogeneity in the drug response, but rather groups the data by similarity in spectral features. Figure 4A-C indicates that each group has a distinct spectral signature that is highly reproducible for all cells within that group and for both drug concentrations that were used. These unique, reproducible Raman spectral signatures can be used for time-resolved monitoring of the different stages of cellular development during drug-induced apoptosis.

Figure 5 shows changes in the Raman spectra for each group (red spectra) compared to the spectrum of untreated (control) cells (blue spectra). A change in Raman peak intensity is indicated with black arrows (pointing up - increase, pointing down - decrease) and the molecular assignment of the peak is provided by a letter code (L - lipid, P - protein, D - DNA). In general, the major changes in the Raman spectra for the individual groups can be attributed to an increase of lipid signal in group 1 (e.g. 1266, 1303, 1445, 1656, 1740 cm^{-1}), an increase of DNA signal in group 2 (e.g. 785, 1094, 1215, 1254, 1378, 1578 cm^{-1}), and a decrease of DNA signal (e.g. 785, 1092, 1340, and 1578 cm^{-1}) accompanied by an increase in protein (Phe – Phenylalanine, 1004 cm^{-1}) signal for group 3.

#135484 - $15.00 USD Received 29 Sep 2010; revised 6 Oct 2010; accepted 7 Oct 2010; published 11 Oct 2010

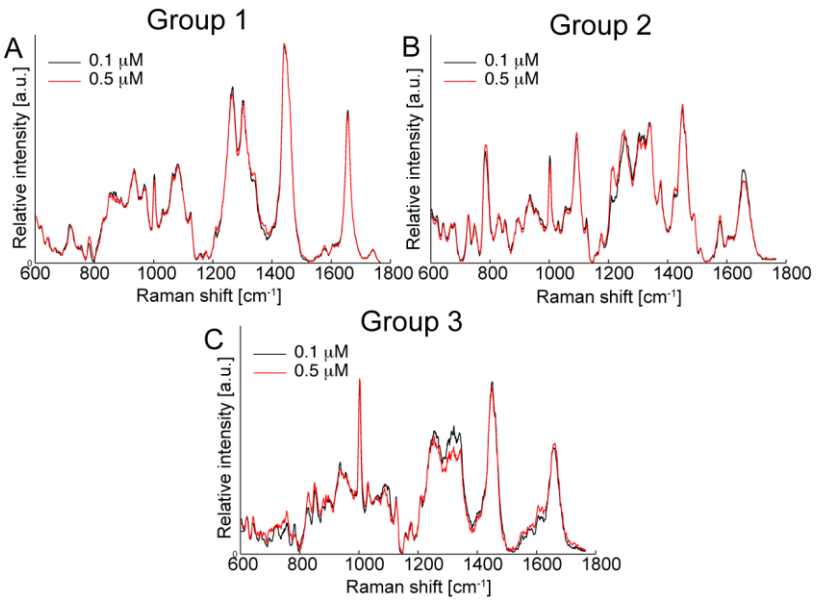

Fig. 4. Mean Raman spectra of the cells in (A) Group 1, (B) Group 2, and (C) Group 3.

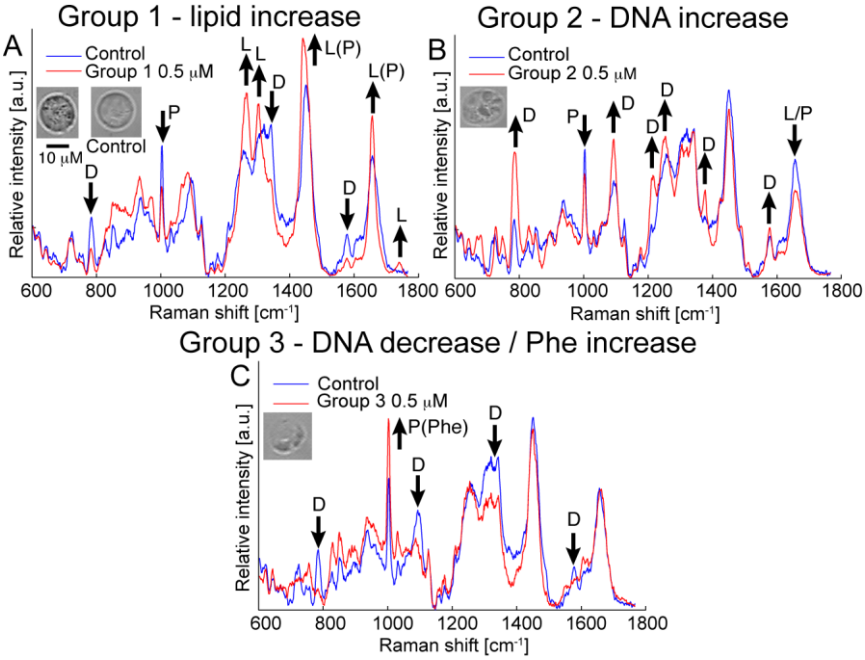

Fig. 5. Comparison of mean Raman spectra from (A) Group 1 (B) Group 2 and (C) Group 3 with the mean Raman spectra of control cells to visualize major spectral changes over time during drug cell interaction. An arrow pointing up or down indicates an increase or decrease in the peak, respectively, and peak assignments are provided: lipid (L), DNA (D), and protein (P). White light images of cells representative of each group and control cells are also shown.

In some cases, morphological changes of the cells could also be observed with white light microscopy. Representative images of drug-exposed cells exhibiting spectra from each of the three groups are also shown in Fig. 5. Also shown is an image of an untreated control cell for comparison. The image assigned to group 1 (Fig. 5A) displays an accumulation of dark spots

#135484 - $15.00 USD Received 29 Sep 2010; revised 6 Oct 2010; accepted 7 Oct 2010; published 11 Oct 2010

within the cell that, considering the increased lipid related Raman signals, could indicate the presence of intracellular vesicles. This observation is consistent with the formation of lipid vesicles at the cell surface (e.g. phosphatidylserine, granule) [26] as well as blebbing of the cell membrane [27] that is known to occur during early stages of apoptosis of leukemic T-lymphocytes (Jurkat) cells induced by doxorubicin [28–31]. Increase in the DNA specific Raman signals in group 2 (Fig. 5B) can be associated with chromatin condensation and nuclear fragmentation as part of the apoptosis process [32–34]. Since Raman signal intensities have a linear dependence on the concentration of molecular bonds in the laser interrogation focal volume, an increase in DNA density due to chromatin condensation would lead to an increase in the DNA peak intensities in the Raman spectra. The cell image in Fig. 5B shows dark regions in the cell that could indicate the formation of dense nuclear fragments. The decrease in intensity of DNA specific Raman peaks and increase in intensity of protein (phenylalanine) specific Raman peaks in the spectrum of group 3 (Fig. 5C) reflects the late stages of apoptosis where nuclear fragments are expelled from the cell leaving an empty shell of cellular membrane and cytoplasm (i.e. a dead cell). The cell image in Fig. 5C shows weak structural contrast, which coincides with this suggested apoptotic phase. The Raman spectra of the three groups in Fig. 5C are remarkably consistent with those of lipid vesicles (granules), nucleus, and cytoplasm of T lymphocytes, as reported in a Raman structural study of granules in lymphokine activated killer (LAK) cells and leukemic cells by Takai *et al.* [35]. A strong increase in DNA specific Raman bands has also been previously reported in taxol induced apoptosis of HeLa cells [17]. Moreover, spectral changes in lipid and DNA Raman bands consistent with the appearance of lipid vesicles at early stages of apoptosis and DNA condensation were also reported in a recent study [18] investigating apoptosis of breast cancer cells induced by etoposide using live cell Raman imaging over 6 h. Changes in DNA and protein associated Raman peaks of drug exposed cells have also been reported in other studies [14–16].

Our previous investigations using laser tweezers Raman spectroscopy (LTRS) of T lymphocytes [24,36] showed remarkable cell-to-cell reproducibility in the Raman spectra presumably due to the large ratio of the nuclear to cytoplasmic volume, which allowed for the nucleus to be probed and trapped consistently. However, the morphological changes that occur during cellular apoptosis may change the optical trapping behavior of the cell, which in turn would contribute to the Raman spectral changes. For example, the accumulation of large quantities of lipid vesicles in the cell may influence the laser trap to preferentially trap those particles leading to a dominant lipid specific Raman signature. We also suggest two mechanisms by which the increase in nuclear density induced by chromatin condensation may lead to an increase in DNA specific Raman signals. The relatively large, dense nuclear fragments could be repositioned to the center of the optical trap, thereby greatly reducing spectral contributions of other parts of the cell. The increased concentration of DNA molecules also could result in stronger DNA specific Raman signals. Additional studies are planned to further investigate the relationship between the morphological changes and the optical trapping behavior of the cell and their influence on the cell spectra.

The potential of inducing cell photodamage using LTRS is always a concern given the laser intensities that are typically used [37]. In our studies however, no laser induced spectral changes were observed at the wavelength, power, and integration time that were used. This is consistent with other studies that have used near infrared (785 nm) LTRS to probe red blood cells [20], or a 660 nm laser to probe human lymphocytes and chromosomes [38]. Moreover, Zoladek *et al.* [18] did not report photodamage issues in their time-course Raman imaging studies of apoptotic cells over 6 hours using approximately the same excitation conditions as in this study. This does not eliminate the possibility that photodamage could still occur if a single cell is continuously interrogated over the course of 72 hours. In depth studies will need to be performed to investigate the dependence of the long-term viability of these cells on the total exposure time and laser intensities that are used.

#135484 - $15.00 USD Received 29 Sep 2010; revised 6 Oct 2010; accepted 7 Oct 2010; published 11 Oct 2010

4. Conclusions

The use of LTRS to monitor the apoptotic response of leukemic T lymphocytes to chemotherapeutical drug treatment was demonstrated. The remarkable reproducibility of the Raman spectral evolution (starting with group 1 and ending with group 3) with exposure time and drug concentration suggests that LTRS, despite not providing a full spatial map of the biochemical components in the cell, is a viable technique for real-time monitoring of biochemical changes associated with apoptosis in individual suspension cells for potential clinical and pharmaceutical applications needing an *in-vitro* chemosensitivity assay for evaluating the efficacy of chemotherapy drug regimens. In this study, LTRS was especially important in order to physically capture the suspension cells, which do not naturally adhere to surfaces, for Raman analysis. In addition, it offers the convenience and simplicity for sampling many cells in solution without requiring extensive sample preparation, such as the need to modify surfaces to promote cell adhesion. We acknowledge that future studies will benefit from the use of dual beam LTRS systems [39] that use one laser beam to trap the cell while a second beam can probe different regions of the cell to obtain a Raman map of the cell or to obtain a spectrum more representative of the entire cell volume. The integration of microfluidic systems [40–43] and multi-focal LTRS (M-LTRS) designs [44] is also expected to be an important development for this technology to enable large populations of individual cells to be rapidly sampled and continuously monitored while maintaining fine control of their chemical environment.

Acknowledgments

This work has been supported by funding from the National Science Foundation. The Center for Biophotonics, an NSF Science and Technology Center, is managed by the University of California, Davis, under Cooperative Agreement No. PHY 0120999. This work was also supported by the Keaton Raphael Memorial Foundation and the Children's Miracle Network.

#135484 - $15.00 USD Received 29 Sep 2010; revised 6 Oct 2010; accepted 7 Oct 2010; published 11 Oct 2010